Geological Survey of Japan Cruise Report No. 22, p. 71-83, 1992

V. HEAT FLOW IN THE SOUTH OF THE NOVA-CANTON TROUGH, CENTRAL EQUATORIAL PACIFIC (GH82-4 AREA)

Toshitsugu Yamazaki

Introduction

Recently, many efforts have been made for obtaining high-accuracy heat flow on old lithosphere (Von Herzen *et al.*, 1982; 1989; Davis *et al.*, 1984; Courtney and White, 1986; Detrick *et al*, 1986; Louden *et al.*, 1987; Lister *et al.*, 1990). An important purpose of these works is to define age-dependence of heat flow on old lithosphere and to know when and how the heat flow departs from the theoretical predictions based on the boundary-layer cooling model and the plate cooling model (Lister, 1977; Parsons and Sclater, 1977). Another subject is to understand better the reheating of lithosphere by hotspots. Heat flow can give constraint on the origin of midplate swells.

In this paper, I present nineteen new heat flow data from Mesozoic seafloor in the south of the Nova-Canton Trough, central equatorial Pacific. Previously only a few heat flow data were reported in this area (Halunen and Von Herzen, 1973). The quality of these old data was obscure because they had no description about the environment (topography, sediment thickness, etc.) around the measurement sites which significantly affects surface heat flow (Sclater *et al.*, 1976). I evaluate the effect of topography and sedimentary environment using echo-sounding and seismic reflection profiles around measurement sites, and make an attempt to obtain true heat flow of the study area. I discuss the observed higher heat flow than the theoretical prediction from lithospheric cooling models.

Geological setting

The study area (Fig. V-1) is located just south of the Nova-Canton Trough. The Manihiki Plateau, one of midplate swells in the Pacific, lies south of this area. The Manihiki Plateau is considered to have been created at or near the triple junction between the Pacific, Antarctic, and Farallon plates at about 110 Ma (Winterer *et al.*, 1974; Jackson and Schlanger, 1976). The depth of the ENE-trending Nova-Canton Trough reaches 8000 m in maximum (Fig. V-2). Ridges occur both sides of the trough. The origin of the trough and ridge system has not yet been made clear, although several models have been presented. They are an abandoned spreading ridge (Winterer, 1976), a deep slot associated with a change in spreading direction (Winterer *et al.*, 1974; Rosendahl *et al.*, 1975), and a transform fault as an extension of the Clipperton Fracture Zone (Menard, 1967) or created by the jump of a triple junction (Lar-

Keywords: heat flow, Cretaceous, lithosphere, intraplate volcanism, Central Pacific Basin, Hakurei-Maru, Nova-Canton Trough

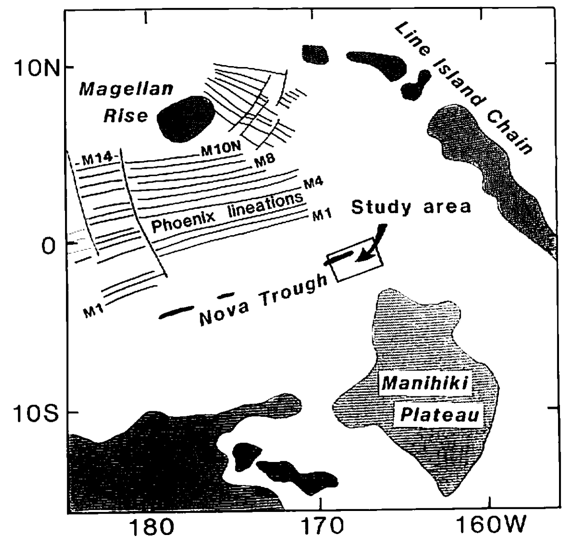

Fig. V-1 Location of the study area (GH82-4 Area) and distribution of magnetic lineations.

son and Chase, 1972).

Mesozoic magnetic lineations known as the Phoenix lineations occur to the northwest of the study area as shown in Figure V-1 (Larson *et al.*, 1972). These lineations indicate that the age of the seafloor becomes young southward. The southernmost lineation identified corresponds to Chron M1R (127.5 Ma, Harland *et al.*, 1990). The seafloor of the study area is thus younger than Chron M1 and older than the age of the Manihiki Plateau, that is, between 110 to 127 Ma, although magnetic lineation correlative to Chron M0 (C34R) has not been found yet. No magnetic lineations which can be correlated to the magnetic reversal time scale are observed in the study area (Yamazaki and Tanahashi, chapter II of this volume). This area would belong to the earliest part of the Cretaceous Magnetic Quiet Zone.

Many deep-sea hills and small seamounts are scattered in the study area. The depth of the eastern half of the study area is slightly shallower than the western half. Twenty heat flow sites are located on gentle slopes or small basins at depths between 5200 to 5800 m. Heat flow was measured at eight sites in the detailed survey area (50 × 40 km) located in the northeastern corner of the GH82-4 area (Fig. V-3).

Measurements

Thermal gradient

Two units of GH80-1 Type thermograd-meter (Matsubayashi, 1982), which has three thermistors each, were used simultaneously at each measurement. A pair of thermistors (one for each apparatus) was attached at the same position to calibrate the two apparatus. Thus temperatures at five different depths in the sediments can be obtained in maximum. Thermistors were mounted at 1 to 1.5 m intervals on the 8-m core barrel in outrigger fashion. Temperature of each thermistor in sediments was measured rela-

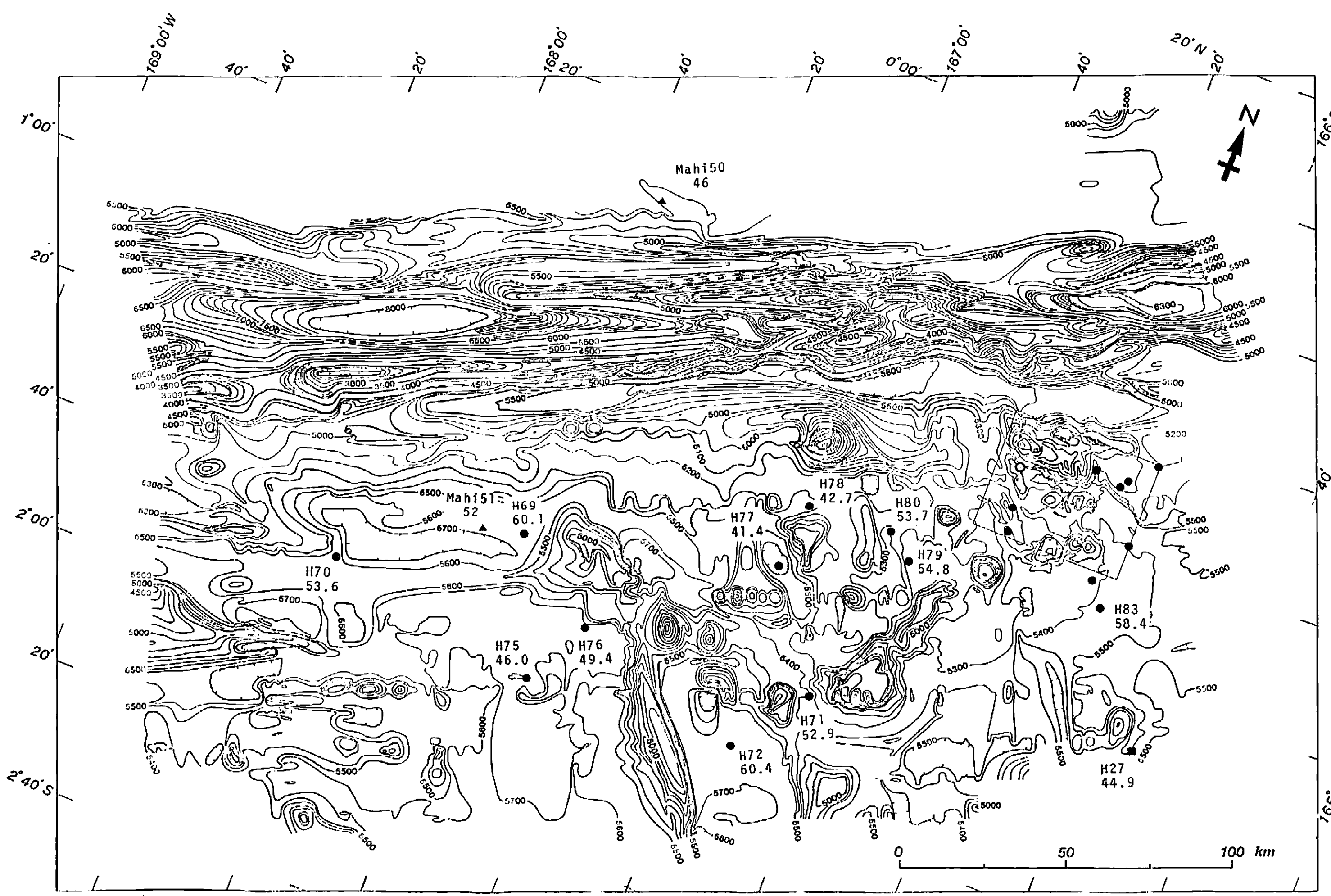

Fig. V-2 Topography and heat flow (mW/m^2) in the study area. A box is the detailed survey area shown in Fig. V-3. Circles represent the sites of heat flow measurement (an open circle was unsuccessful one), triangles the data from Halunen and Von Herzen (1973) and a square from Matsubayashi (1982). Contour interval is 100 m.

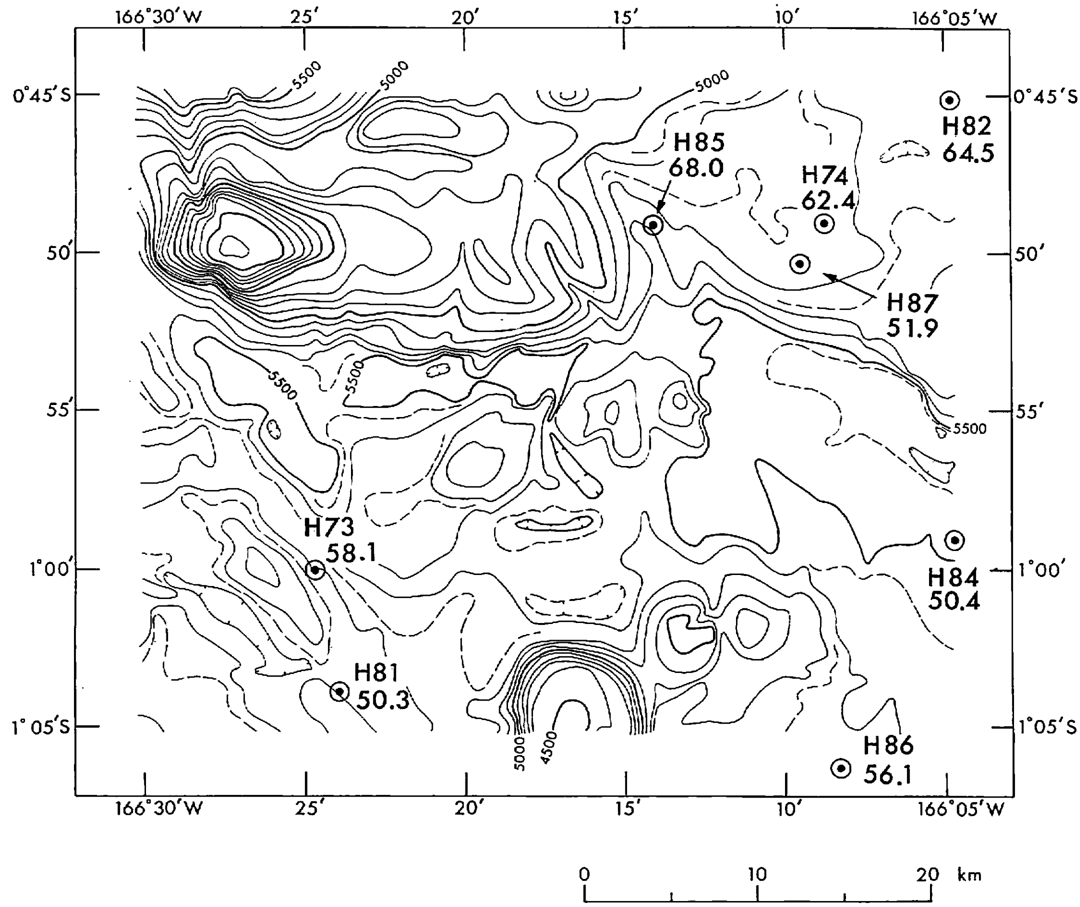

Fig. V-3 Heat flow (mW/m^2) and topography of the detailed survey area (boxed in Fig. V-2). Topographic contours are at 100 m intervals.

tive to bottom-water temperature obtained at about 30 m above the seafloor immediately after pulling out from the sediments. Decay of frictional heating of the thermistors during penetration into sediments was monitored for 10 minutes. The frictional heating was usually very small because of hydrous nature of the sediments. The accuracy in temperature difference is within 0.01 °C.

An average thermal gradient was calculated by fitting a straight line on depth-temperature plots using the least-squares method. Nice linearity of thermal gradient is shown at all sites (Fig. V-4). The absolute depth of each thermistor in sediments is unknown due to difficulty to measure accurate penetration depth of a corer. The figure is drawn assuming full penetration of an 8-m long core barrel, which is reasonable from the length of the recovered sediment core and mud adhered to the core barrel. If the thermal gradient and thermal conductivity are constant between the uppermost thermistor and sediment-water interface, overpenetration of 1 m or less must have

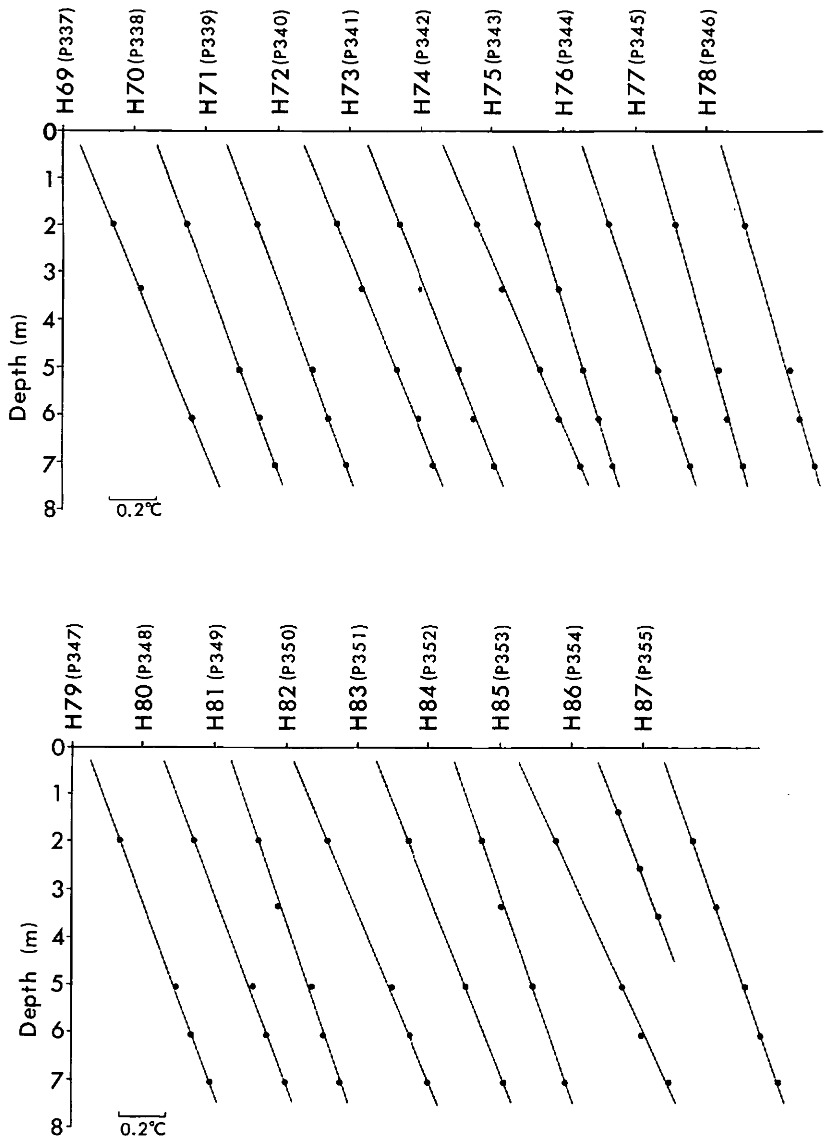

Fig. V-4 Temperature profiles in the sediments. Temperature differences from the temperature of bottom water just above seafloor are indicated. Thermal gradient was calculated by fitting a straight line using the least-squares method.

occurred.

Thermal conductivity

Thermal conductivity of half-split cores was measured using QTM (Quick Thermal conductivity Meter, manufactured by Showa Denko Co.) at intervals of 30 to 50 cm. Detailed descriptions of measurement by the QTM were given in Horai (1982). Cores were split into halves immediately after recovery, and covered with thin plastic film to prevent dehydration. Measurements were done on board as soon as the thermal steady state was attained at about 25°C in several hours after recovery. The effect of the plastic film is negligible, which was confirmed by measuring standard (fused quartz).

The thermal conductivity data after correction for the effects of in situ temperature and pressure (Ratcliffe, 1960) are plotted with depth in Figure V-5. Samples are composed mostly of siliceous clay or ooze because water depths of the study area have been below the Carbonate Compensation Depth (CCD), which is about 5000 m at present (Berger and Winterer, 1974). Several cores, however, are intercalated by a few thin layers of calcareous turbidite. Scattered high conductivity values in Figure V-5 correspond to the calcareous turbidite layers, and uniform low values of about 0.75 W/mK are values of siliceous clay or ooze. The effect of the high conductivity layers is too small to be seen on the corresponding thermal gradient data because the thickness of the high-conductivity layers is only in the order of 10 cm. Claystone of H68 (P336) has higher thermal conductivity (0.8 to 0.9 W/mK) than that of siliceous clay, which would probably be caused by its lower porosity. No thermal gradient data was obtained at this site.

Effect of topography and sedimentary environment

Results of heat flow measurements are summarized in Table V-1. Simple mean and standard deviation of the nineteen heat flow values are $54.5 \pm 6.9 \ mW/m^2$.

Local sedimentary environment of each heat flow sites was evaluated using seismic reflection and topographic profiles. The sites were classified using the Environment Quality Factor (E.Q.F.) proposed by Sclater *et al.* (1976). The definition of E.Q.F. is as follows (Anderson *et al.*, 1977): rank A, generally thick and uniform sediment cover draping all basement relief with no outcrops within 10 km of the measurement site; rank B, thick sediments but with isolated basement outcrops within 10 km of the site; rank C, rough topography with a thin sediment cover usually less than 100 m over most basement relief. The basement of this area is, in general, covered with thick sedimentary layer due to its fairly old age (older than 110 Ma). In regions of rough topography such as deep-sea hills or cliffs, however, a part of basement has only thin sedimentary layer or may be exposed. Only four sites out of nineteen are classified to the rank A of E.Q.F. The mean heat flow of these four sites, which are considered to be most reliable, is $59.9 \ mW/m^2$. This value is higher than the mean of other sites, $53.0 \ mW/m^2$. Reduction of surface heat flow by water circulation through thin "impermeable" sedimentary layer, which is known to be common on young oceanic crust (Lister, 1972), may occur even in the regions underlain by Mesozoic basement.

I evaluate the effect of topography on some of the heat flow sites, and show that

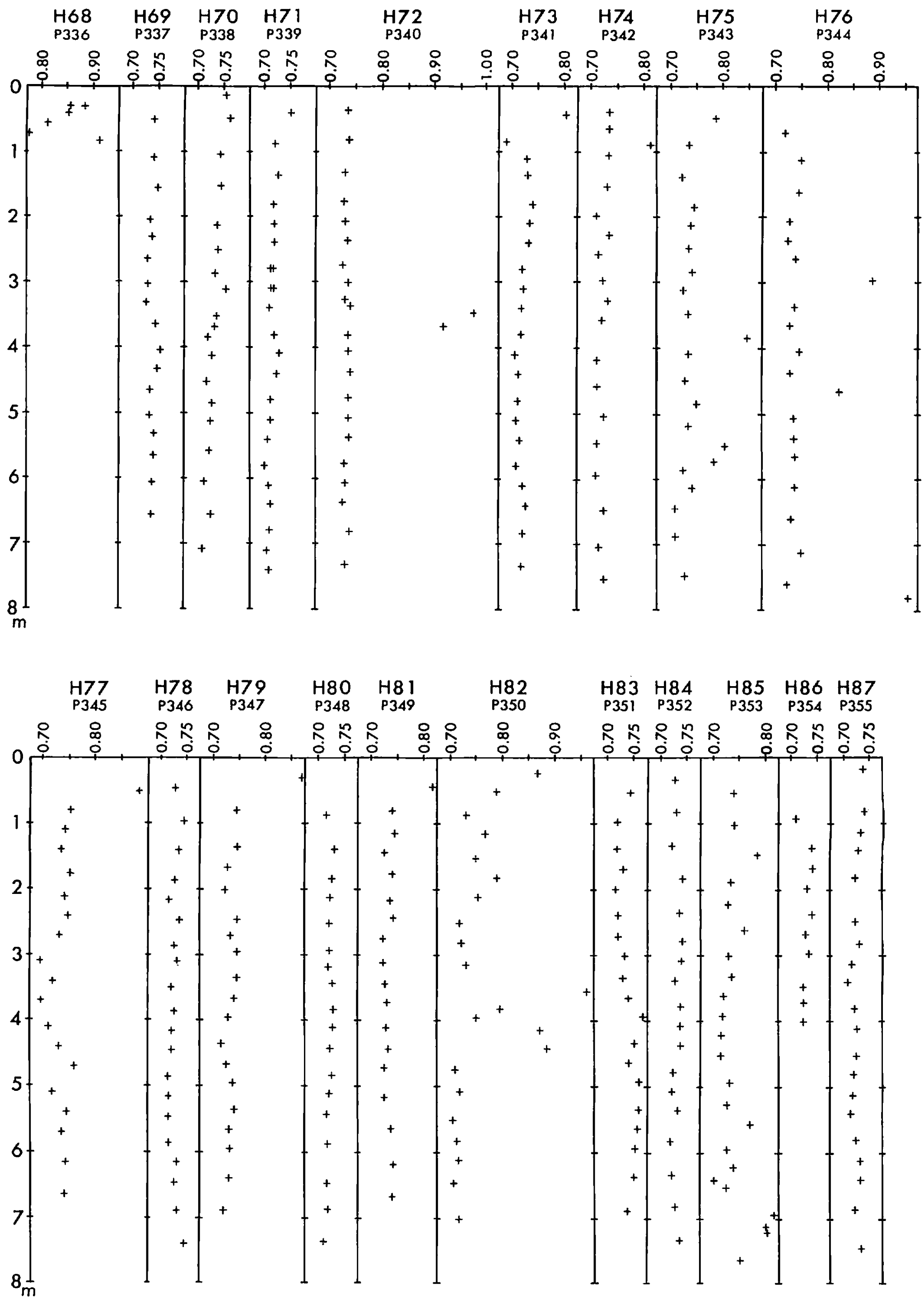

Fig. V-5 Thermal conductivity with depth measured on cored sediments.

reliable heat flow of the study area can be represented by the mean of the rank A sites in E.Q.F. I used a method proposed by Matsubayashi (1983) for numerical calculation of the effect of topography. This method adopts the boundary element method (BEM) for solving numerically an integral equation being transformed from the Laplace's equation by the Green's formula.

This technique was applied to the topography around the sites (a) H74 and H87, and (b) H85. The topography is treated as two dimensional linear elements for simplicity as shown in Fig. V-6. I used following boundary conditions: (1) temperature at the sea floor is constant, which is justified by the fact that the thermal gradient of the bottom water of this area is negligibly small (Yamazaki, chapter XIII of this volume), (2) thermal gradient at 10 km below the sea level is constant, *C*, and (3) no heat flows through vertical boundaries. Figure V- 6 shows the ratio of calculated thermal gradient at the topographic surface to *C*, the given boundary condition.

Despite short distance of about 5 km between the two sites, H74 and H87, measured heat flow value at H87 (51.9 mW/m^2), is apparently (about 17%) lower than that at H74 (62.4 mW/m^2). About a half of the observed difference can be explained by the effect of the topography (Fig. V-6a). Another half may be explained by that pore-water movement through the steep slope south of H87 where thin or no sediment cover develops reduced the surface heat flow. Thus the observed value at H74 serves more reliable heat flow than that at H87.

The highest heat flow in the study area was 68 mW/m^2 at H85. However the effect of topography would cause an about 15% growth of the surface heat flow (Fig. V-6b). The true heat flow at H85 can hence be estimated to be about 60 mW/m^2.

These two examples of the topographic effect support the consideration that the true heat flow of this area can be represented as about 60 mW/m^2 by the mean of the rank-A sites in E.Q.F.

Discussion: heat flow higher than theoretical predictions

I compare the observed heat flow with theoretical predictions based on lithospheric cooling models. The age of the seafloor of the study area is considered to be between 110 to 127 Ma. Thus the maximum predicted heat flows are 45.1 mW/m^2 according to the boundary layer model for 110 Ma, and 49.1 mW/m^2 according to the Plate model (Lister, 1977; Parsons and Sclater, 1977). The mean heat flow of high quality sites (60 mW/m^2), which represent reliable heat flow of this area, is significantly higher than these predictions. The mean of all sites including ones of poor environmental condition (55 mW/m^2) is still a little higher than the predictions.

Heat flows higher than expected from lithospheric cooling models were often observed on or close to midplate swells, and were interpreted to be caused by reheating of the lithosphere by hotspots (Von Herzen *et al.*, 1982; Davis *et al.*, 1984; Courtney and White, 1986; Detrick *et al.*, 1986; Louden *et al.*, 1987). Recent detailed heat flow measurements, however, reveals that heat flows off midplate swells are still higher than the prediction by the models (Von Herzen *et al.*, 1989; Lister *et al.*, 1990). They considered that heat flow associated with midplate swells would be less than previously thought, and the swells would be supported dynamically. Lister *et al.* (1990) considered that many relatively weak localized sources of heat would be needed to explain the heat

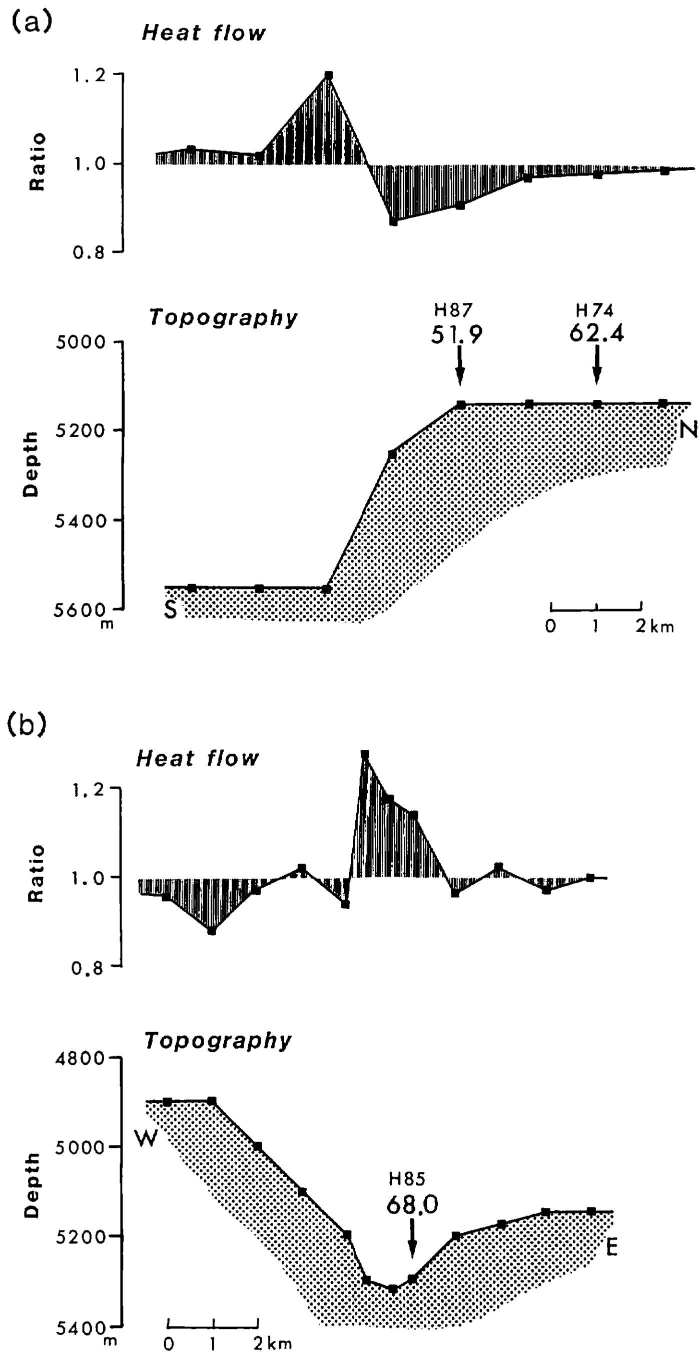

Fig. V-6 Simplified topographic profile (bottom), and the ratio of the calculated thermal gradient at the surface to the gradient given as a boundary condition at 10 km below the sea level (top). Sites (a) H74 and H87, and (b) H85.

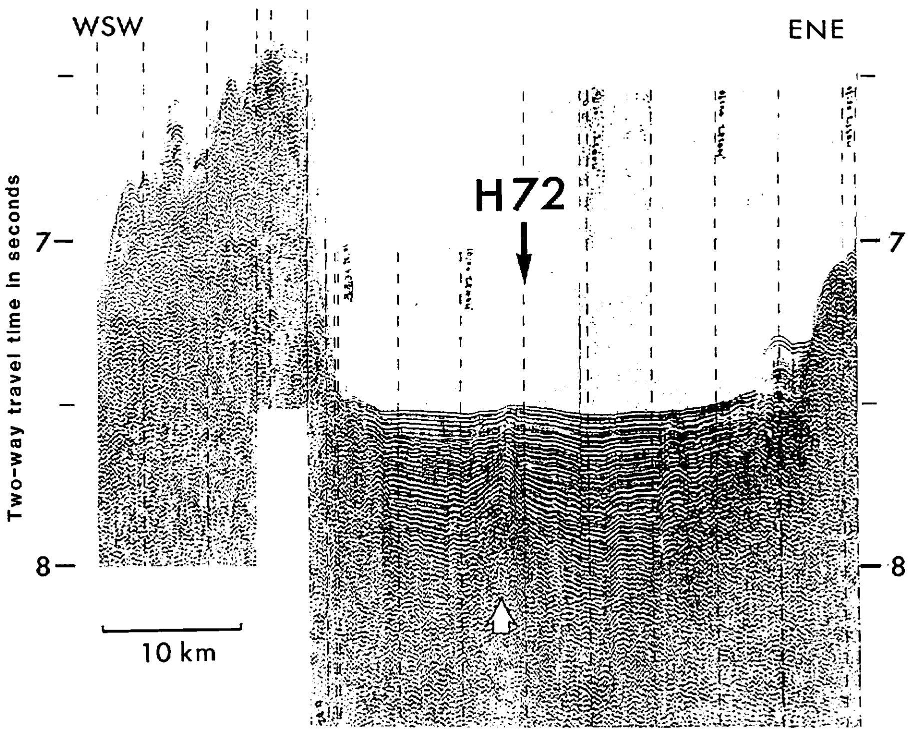

Fig. V-7 Seismic reflection profiles across site H72. Note an intrusion in the basin filled with turbidites (white arrow).

flow higher than expected.

The study area is located north of the Manihiki Plateau. This area was, however, not affected by volcanism which formed the plateau because its water depth (5200 to 5800 m) is not shallower than those of other areas having similar ages. On the other hand, seismic reflection profiles provide some evidence for occurrence of tectonic activity after the creation of the seafloor (Tanahashi, chapter IV of this volume). Some basins in the southwestern part of the study area which are filled with turbidites have peaks of acoustic basement. An example is presented in Figure V-7, which is close to site H72. Deformation of the turbidite layers which can be recognized in this figure suggests that the basement high would be an igneous intrusion which occurred during deposition of the turbidites. Deep-sea hills scattered in this area may have been formed by structural movements after the deposition of thick acoustically semi-opaque layers which is estimated to be limestone and chart of Cretaceous to Eocene age (Tanahashi, chapter IV of this volume). Thus it would be possible to consider that the heat associated with these postdated tectonic activities causes the observed higher heat flow than the theoretical prediction.

Table V-1 Summary of heat flow measurements.

Station	Latitude (S)	Longitude (W)	Depth (m)	EQF	N	G (10^{-2}K/m)	K (W/mK)	Q (mW/m^2)
H68 (P336)	0°53.63'	166°25.77'	5434	C	0		0.850±0.042	
H69 (P337)	1°32.97	167°36.36'	5667	B	3	8.12	0.740±0.007	60.1
H70 (P338)	1°47.70'	168°03.61'	5537	B	4	7.31	0.733±0.014	53.6
H71 (P339)	1°40.52'	166°44.32'	5403	C	4	7.37	0.718±0.010	52.9
H72 (P340)	1°52.67'	166°53.31'	5687	A	5	8.24	0.733±0.005	60.4
H73 (P341)	1°00.05'	166°24.68'	5377	B	5	8.03	0.723±0.021	58.1
H74 (P342)	0°49.18'	166°08.68'	5174	B	5	8.57	0.728±0.022	62.4
H75 (P343)	1°54.65'	167°27.55'	5791	B	5	6.17	0.746±0.033	46.0
H76 (P344)	1°43.48'	167°21.77'	5791	B	4	6.72	0.735±0.009	49.4
H77 (P345)	1°22.65'	166°56.40'	5648	C	4	5.60	0.740±0.038	41.4
H78 (P346)	1°11.87'	166°55.25'	5323	B	4	5.88	0.726±0.009	42.7
H79 (P347)	1°14.37'	166°37.33'	5169	B	4	7.40	0.741±0.032	54.8
H80 (P348)	1°10.83'	166°41.65'	5292	B	4	7.45	0.721±0.005	53.7
H81 (P349)	1°03.94'	166°23.94'	5309	B	5	6.82	0.738±0.021	50.3
H82 (P350)	0°45.17'	166°04.76'	5219	A	4	8.41	0.767±0.069	64.5
H83 (P351)	1°10.01'	166°05.35'	5382	A	3	7.90	0.739±0.015	58.4
H84 (P352)	0°59.05'	166°04.70'	5517	B	4	6.90	0.730±0.008	50.4
H85 (P353)	0°49.07'	166°14.03'	5249	B	4	9.14	0.744±0.031	68.0
H86 (P354)	1°06.33'	166°08.23'	5353	A	3	7.67	0.731±0.010	56.1
H87 (P355)	0°50.34'	166°09.43'	5164	B	5	7.14	0.727±0.008	51.9

EQF : Environment Quality Factor after Sclater et al. (1976).
N : Number of active thermistors in sediments.
G : Thermal gradient.
K : Thermal conductivity.
Q : Heat flow.

Summary

Nineteen new heat flow values were obtained in the south of the Nova-Canton Trough, central equatorial Pacific. The age of the seafloor is between 110 and 127 Ma. The mean heat flow, 60 mW/m^2, of the high quality sites which are classified to the rank A of E.Q.F. of Sclater *et al.* (1977) is higher than the mean, 53 mW/m^2, of other sites (the ranks B or C). The effect of topography was evaluated using the boundary element method. The results support the consideration that the true heat flow is represented by the four sites of rank A. The heat flow of this area is significantly (more than 10 mW/m^2) higher than the predictions from the theoretical lithospheric cooling models for 110 Ma. Seismic reflection profiles suggest that some igneous activities and tectonic movements occurred after the creation of the seafloor, which would be responsible for the heat flow higher than the theoretical prediction.

Acknowledgements

The author is much indebted to O. Matsubayashi who provided me a computer program of the boundary element method and gave useful suggestion.

References

Anderson, R. N., Langseth, M. G. and Sclater, J. G. (1977) The mechanisms of heat transfer through the floor of the Indian Ocean. *J. Geophys. Res.*, vol. 82, p. 3391–3409.

Berger, W. H. and Winterer, E. L. (1974) Plate stratigraphy and the fluctuating carbonate line. *Intl. Assoc. Sedimentologists Spec. Pub.*, vol. 1, p. 11–48.

Courtney, R. C. and White, R. S. (1986) Anomalous heat flow and geoid across the Cape Verde Rise: evidence for dynamic support from a thermal plume in the mantle. *Geophys. J. R. astr. Soc.*, vol. 87, p. 815–867.

Davis, E. E., Lister, C. R. B. and Sclater, J. G. (1984) Towards determining the thermal state of old ocean lithosphere: heat-flow measurements from the Blake-Bahama outer ridge, north-western Atlantic. *Geophys. J. R. aster. Soc.*, vol. 78, p. 507–545.

Detrick, R. S., Von Herzen, R. P., Parsons, B., Sandwell, D. and Dougherty, M. (1986) Heat flow observations on the Bermuda Rise and thermal models of midplate swells. *J. Geophys. Res.*, vol. 91, p. 3701–3723.

Halunen, A. J. and Von Herzen, R. P. (1973) Heat flow in the Western Equatorial Pacific Ocean. *J. Geophys. Res.*, vol. 78, p. 5195–5208.

Harland, W. B., Armstrong, R. L., Cox, A. V., Craig, L. E., Smith, A. G. and Smith, D. G. (1990) *A geologic time scale 1989.* Cambridge University Press, Cambridge, 263 p.

Horai, K. (1982) Thermal conductivity of sediments and igneous rocks recovered during Deep-Sea Drilling Project Leg 60. In: Hussong, D., Uyeda, S. *et al.* (eds.), *Init. Rept. DSDP*, vol. 60, U.S. Govt. Printing Office, Washington, D.C., p. 807–834.

Jackson, E. D. and Schlanger, S. O. (1976) Regional syntheses, Line Islands Chain, Tuamotu Island Chain, and Manihiki Plateau, central Pacific ocean. In: Schlanger, S. O., Jackson, E. D., *et al.* (eds.), *Init. Rept. DSDP*, vol. 33, U.S. Govt. Printing Office, Washington, D.C., p. 915–927.

Larson, R. L. and Chase, C. G. (1972) Late Mesozoic evolution of the Western Pacific Ocean. *Geol. Soc. Amer. Bull.*, vol. 83, p. 3627–3644.

———, Smith, S. M. and Chase, C. G. (1972) Magnetic lineations of early Cretaceous age in the western equatorial Pacific ocean. *Earth Planet. Sci. Lett.*, vol. 15, p. 315–319.

Lister, C. R. B. (1972) On the thermal balance of a mid-ocean ridge. *Geophys. J. R. astr. Soc.*, vol. 26, p. 515–535.

——— (1977) Estimations for heat flow and deep rock properties based on Boundary Layer theory. *Tectonophysics*, vol. 41, p. 157–171.

———, Sclater, J. G., Davis, E. E., Villinger, H. and Nagihara, S. (1990) Heat flow maintained in ocean basin of great age: investigations in the north-equatorial West Pacific. *Geophys. J. Int.*, vol. 102, p. 603–630.

Louden, K. E., Wallace, D. O. and Courtney, R. C. (1987) Heat flow and depth versus age for the Mesozoic northwest Atlantic Ocean: results from the Sohm abyssal plain and implications for the Bermuda Rise. *Earth Planet. Sci. Lett.*, vol. 83, p. 109–122.

Matsubayashi, O. (1982) Reconnaissance measurements of heat flow in the Central Pacific. *Geol. Surv. Japan Cruise Rept.*, no. 18, p. 90–94.

——— (1983) Application of boundary element technique to evaluation of topographic effect on heat flow observation. *J. Geotherm. Res. Soc. Japan*, vol. 5, p. 249–257.

Menard, H. W. (1967) Extension of northeastern-Pacific fracture zones. *Science*, vol. 155, p. 72–74.

Parsons, B. and Sclater, J. G. (1977) An analysis of the variation of ocean floor bathymetry and heat flow with age. *J. Geophys. Res.*, vol. 82, p. 803–827.

Ratcliffe, E. H. (1960) The thermal conductivities of ocean sediments. *J. Geophys. Res.*, vol. 65, p. 1535–1541.

Rosendahl, B. R., Moberly, R., Halunen, J. A., Rose, J. C. and Kroenke, L. W. (1975) Geological and geophysical studies of the Canton Trough region. *J. Geophys. Res.*, vol. 80, p. 2565–2574.

Sclater, J. G., Crowe, J. and Anderson, R. N. (1976) On the reliability of ocean heat flow averages. *J. Geophys. Res.*, vol. 81, p. 2997–3006.

Von Herzen, R. P., Detrick, R. S., Crough, S. T., Epp, D. and Fehn, U. (1982) Thermal origin of the Hawaiian Swell: Heat flow evidence and thermal models. *J. Geophys. Res.*, vol. 87, p. 6711–6723.

———, Cordery, M. J., Detrick, R. S. and Fang, C. (1989) Heat flow and the thermal origin of hot spot swells: the Hawaiian Swell revisited. *J. Geophys. Res.*, vol. 94, p. 13783–13799.

Winterer, E. L. (1976) Anomalies in the tectonic evolution of the Pacific. In: Sutton, G. H., Manghnani, M. H., Moberly, R. and Mcafee, E. U. (eds.), *The geophysics of the Pacific Ocean Basin and its margin, Geophysical Monograph* no. 19, American Geophysical Union, Washington, D.C., p. 269–278.

———, Lonsdale, P. F., Matthews, J. L. and Rosendahl, B. R. (1974) Structural and acoustic stratigraphy of the Manihiki Plateau. *Deep-Sea Res.*, vol. 21, p. 793–814.